Computational Study of Arzanol – an Antioxidant Compound of Natural Origin

Liliana Mammino

***Abstract*—** Arzanol is a naturally-occurring biologically active acylphloroglucinol isolated from *Helichrysum italicum*. It exhibits anti-oxidant, antibiotic and antiviral activities. The current work presents the results of a computational study of arzanol, aimed at identifying conformational preferences and other interesting molecular characteristics. Calculations *in vacuo* were performed at the HF and DFT levels of theory with full optimization (fully relaxed geometry) and at the MP2 level as single-point calculations on HF-optimized results. Calculations in solution were performed with the Polarisable Continuum Model, at the HF level, considering three different solvents – chloroform, acetonitrile and water. The results show that only one conformer is populated in all the media – the conformer comprising all the stabilizing effects, among which the presence of three intramolecular hydrogen bonds plays dominant role. The results also show good consistency with the general trends identified for acylphloroglucinols, both *in vacuo* and in solution.

***Keywords*—**Acylphloroglucinols, Antioxidants, Arzanol, Intramolecular hydrogen bonding, Polyphenols.

I. Introduction

ARZANOL ($C_{22}H_{26}O_7$) is a prenylated phloroglucinyl α-pyrone. Its structure is shown in fig. 1, together with the atom numbering utilized in this work. It is a biologically active compound of natural origin, and is the major responsible of the anti-inflammatory, anti-oxidant, antibiotic and antiviral activities of *Helichrysum italicum* [1–3].

Arzanol belongs to the class of acylphloroglucinols (ACPL) – derivatives of phloroglucinol (1,3,5-trihydroxybenzene) characterized by the presence of a COR group (acyl chain). ACPL, in turn, belong to the broader class of polyphenols – a class including many compounds with antioxidant activity.

A comparison with the general structure of ACPL (fig. 2) shows that, in arzanol, R is a methyl, R′ is the α-pyrone ring bonded to the phloroglucinol ring through a methylene bridge, and R″ is a prenyl chain.

In general, the biological activity of polyphenols is tightly related to their molecular characteristics [4]–[6]. Furthermore, a detailed knowledge of the molecular properties of a biologically active compound is essential for the objective of designing derivative molecules with more potent activity [7].

Manuscript received January 31, 2012: Revised version received .....

L. Mammino is with the Department of Chemistry, University of Venda, Thohoyandou 0950, South Africa (corresponding author; phone: +27-15-962-8147; fax: +27-15-962-4749; e-mail: sasdestria@yahoo.com).

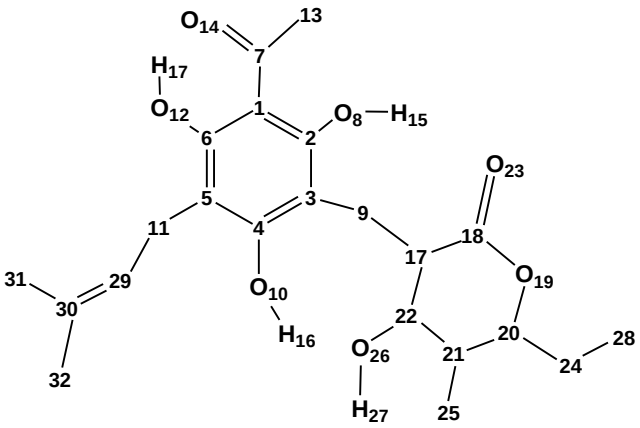

Fig. 1. Structure of the arzanol molecule and atom numbering utilized in this work.
The figure shows the carbon skeleton of the molecule, the O atoms, and the H atoms pertaining to OH groups. The other H atoms are hidden, to better highlight the molecular structure. The C atoms are denoted by their numbers.
The phloroglucinol moiety is oriented in the same way as the general structure in fig. 2, to facilitate the identification of correspondences.

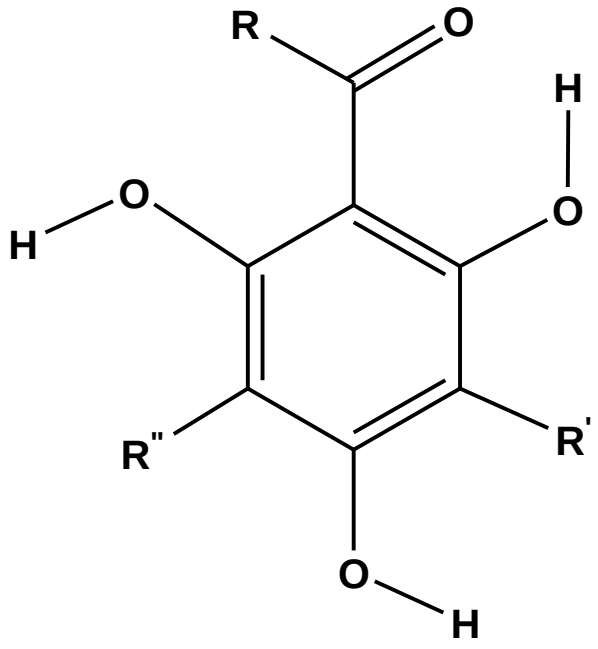

Fig. 2. General structure of acylphloroglucinols.

Antioxidant compounds are of interest in medicine because, by protecting the organism against reactive oxygen species (ROS), they help preventing damages to the central nervous system and the insurgence of neurodegenerative diseases like ischemia, Alzheimer disease, Parkinson disease and schizophrenia [8], [9].

An additional interest for the computational study of the arzanol molecule relates to the fact that its structure is different from the structures of the ACPL investigated so far within a systematic study [10]–[13], because the phloroglucinol moiety is bonded to a moiety of a different nature (pyrone) through a methylene bridge. It is therefore particularly interesting to verify the extent to which the results for arzanol are consistent with the general patterns identified for ACPL and with the predictions that can be based on them.

The current work reports the results of a computational study of the arzanol molecule *in vacuo* and in solution, aimed at:

- identifying its conformational preferences *in vacuo* and in different solvents;
- identifying important aspects of its geometry, such as the parameters of intramolecular hydrogen bonds (IHB);
- comparing its results with the general patterns identified for ACPL.

II. Computational Details

Calculations *in vacuo* were performed at the Hartree Fock (HF) level with the 6-31G(d,p) basis set and at the Density Functional Theory (DFT) level with the 6-31+G(d,p) basis set and the B3LYP functional.

The study of ACPL [10]–[13] had shown that HF gives reasonable results for this class of compounds and enables realistic trend-identifications, already with the 6-31G(d,p) basis set. DFT calculations were added to have an additional verification of results. The B3LYP functional is the most widely utilized in molecular calculations [14]. The 6-31+G(d,p) basis set was selected for DFT calculations as the general study of ACPL had shown that the performance of DFT without diffuse functions on the heavy atoms (e.g., with the 6-31G(d,p) basis set) is poor.

All the calculations *in vacuo* were performed with full optimization (fully relaxed geometry), to better identify the details of the geometries corresponding to minima on the potential energy surface. The inputs for HF calculations were prepared on the basis of identified preferences for ACPL. The HF optimized geometries were then utilized as inputs for DFT calculations.

MP2 calculations with relaxed geometry would provide better-quality results, above all for the description of IHB, because MP2 takes into account both electron correlation and dispersion effects, which both contribute to the hydrogen bond interaction. However, full-optimization MP2 calculations were not affordable for a molecule of this size (55 atoms). Single point MP2 calculations were performed on the HF optimized geometries; although they do not improve the parameters of the IHB, single point results are useful for a comparison of the energy trends. The choice of HF optimized geometries as those on which to perform single point MP2 calculation is natural, because the HF calculation constitutes the fist step (providing the "unperturbed" results) in the MP2 algorithm.

Table 1. Symbols (S) utilized to denote the main geometry features of the conformers of arzanol.

S	geometrical feature	S	geometrical feature
d	The first IHB engages H15.	s	The first IHB engages H17.
r	H16 is oriented toward the pyrone group.	w	H16 is oriented toward the prenyl chain.
η	presence of O–H···π interaction between the double bond in the prenyl chain and H16	ξ	presence of O–H···π interaction between the double bond in the prenyl chain and H17

Calculations in solution were performed with the Polarizable Continuum Model (PCM, [15] –[18]) at the HF/6-31G(d,p) level, on the HF *in-vacuo*-optimized geometries and with full reoptimization. The same three solvent utilized in the study of ACPL (chloroform, acetonitrile and water, [13]) were considered, as they cover the range of polarities and H-bond formation abilities of the media in which a biologically active molecule may preferably be present within a living organism.

All the calculations were performed with Gaussian 03, revision D01 [14].

All the energy values reported are in kcal/mol and all the length values are in Å.

III. Results

A. Results in vacuo

The atom numbering utilized in this work (fig. 1) maintains the same numbering utilized for the phloroglucinol moiety in the study of ACPL ([10]–[13]), to facilitate cross-references and comparisons. In addition, the same letters utilized to keep track of relevant geometry features of ACPL ([10]–[13]) are utilized to denote the conformers of arzanol; their meaning is explained in table 1. In the rest of this work, the methyl of the acyl chain is concisely termed R, the substituent at C3 is concisely termed R′ and the prenyl chain at C5 is concisely termed R″, following the correspondence of the structure of the arzanol molecule with the general structure of ACPL (identifiable by comparing fig. 1 and 2).

The calculated conformers comprised all the interesting geometries except those without the first IHB, because the study of ACPL had shown that they have very high relative energy in all the media – well beyond the values that are considered potentially interesting for biological activities. Table 2 reports the relative energies of the calculated conformers, and fig. 3 shows their geometries.

The presence of the pyrone ring and the importance of the simultaneous presence of inter-monomers H-bonds on either side of the methylene bridge drastically reduce the possibility of viable conformers. Conformers with the first IHB engaging

Table 2. Relative energies of the calculated conformers of arzanol in vacuo.
The column titled HF reports the results from full optimization HF/6-31-G(d,p) calculations; the column titled DFT reports the results from full optimization DFT/B3LYP/6-31-G+(d,p) calculations; the column titled MP2 reports the results from single-point MP2/6-31-G(d,p) calculations on HF optimized geometries.

conformer	relative energy (kcal/mol)		
	HF	DFT	MP2
s-w-η	0.0000	0.0000	0.0000
s-r	9.2452	10.0998	10.1166
d-w-η	15.2813	16.6892	16.1523
d-w-ξ	15.8449	17.3083	17.0253
d-r-ξ	15.8593	16.3844	16.6358

H15 (d conformers), usually preferred for ACPL, are not viable for arzanol because they would prevent H15 from forming the intermonomer H-bond with O23. Conformers with the first IHB engaging H17 (s conformers) enable the formation of two intermonomer H-bonds. The s-w-η conformer appears to be the only populated one. The much higher relative energy of the s-r conformer (although maintaining two intermonomer H-bonds) can be ascribed both to the general trend of ACPL, for which it usually has higher relative energy than the s-w conformer, and to the absence of the O–H···π interaction, present in s-w-η and having considerable influence on the conformational preferences of molecules with a π bond in a suitable position in a side chain [12]. The space-filling models of the two conformers (fig. 4) are better apt to highlight the presence or absence of the O–H···π interaction.

Table 3 reports the characteristics of all the IHB (both the first IHB and the intermonomer H-bonds), in the results of the two methods for which calculations were performed with fully relaxed geometry (full optimization); since MP2 calculations were performed as single point, the conformer geometry is the same as in the HF results. The IHB length values in the DFT results are shorter than in the HF results, for the same IHB; this is a known phenomenon with DFT calculations, which tends to overestimate H-bond energies, thus giving shorter H-bond lengths.

The H···O length is an indication of the IHB strength; this, in turn, is an indication of the stabilizing effect of a given IHB. A detailed consideration of the IHB lengths may help understand the large energy gap between the s-w-η conformer and the s-r conformer, and also some destabilizing aspects of the d conformers. The H17···O14 length is shorter in the s-w-η conformer than in the s-r conformer. Differently from what generally observed for ACPL, the H15···O14 length is longer than the H17···O14 length, suggesting that the H15···O14 IHB is somewhat weaker than the H17···O14 IHB. The H15···O23 length is ≈0.038 Å shorter in the s-w-η conformer than in the s-r conformer. The H27···O10 IHB is 0.134/HF and 0.055/DFT Å shorter in the s-w-η conformer than in the d-w-η conformer; it

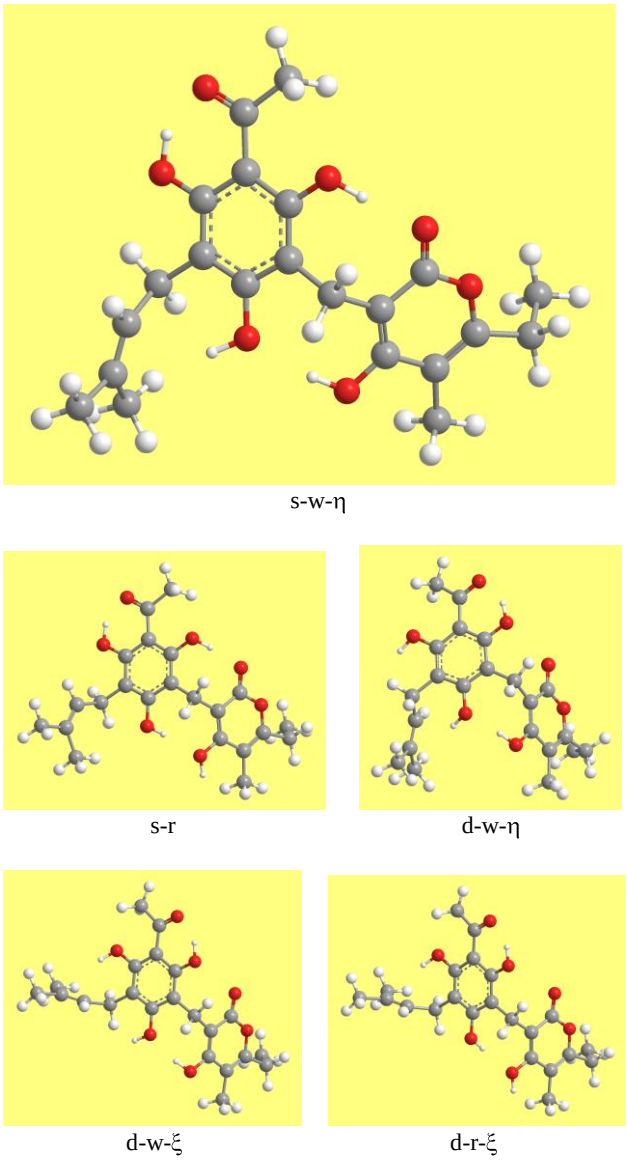

Fig.3. Calculated conformers of arzanol. HF/6-31G(d,p) results *in vacuo*.

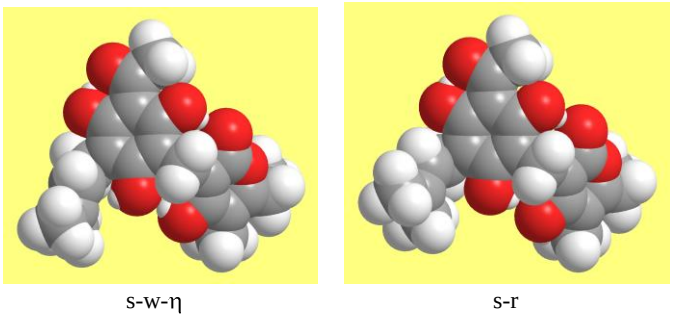

Fig. 4. Space filling models of the two conformers of arzanol in which the first IHB engages H17.
The model of the s-w-η conformer clearly shows the orientation of H16 toward the π bond of the prenyl chain (O–H···π interaction).

Table 3. Characteristics of the intramolecular hydrogen bonds in the calculated conformers of arzanol.
The first column (conf) reports the conformer; the second column (meth) reports the calculation method; the third column (IHB) specifies the IHB considered; the other three columns report the parameters of the IHB: bond length (O···H), O···O distance and bond angle (OĤO). The methods are denoted with the acronyms HF for HF/6-31-G(d,p) calculations and DFT for DFT/B3LYP/6-31-G+(d,p) calculations.

conf	meth	IHB	O···H (Å)	O···O (Å)	
s-w-η	HF	H17···O14	1.658	2.612	150.0
		H15···O23	1.795	2.744	170.9
		H27···O10	1.897	2.826	164.8
	DFT	H17···O14	1.528	2.465	151.6
		H15···O23	1.697	2.682	170.5
		H27···O10	1.797	2.769	169.4
s-r	HF	H17···O14	1.676	2.525	145.5
		H15···O23	1.833	2.773	168.0
		H16···O26	2.040	2.955	162.9
	DFT	H17···O14	1.548	2.478	151.1
		H15···O23	1.733	2.711	170.9
		H16···O26	1.952	2.904	166.8
d-w-η	HF	H15···O14	1.685	2.5527	144.6
		H27···O10	2.031	2.833	141.3
	DFT	H15···O14	1.555	2.478	150.3
		H27···O10	1.852	2.752	151.8
d-w-ξ	HF	H15···O14	1.688	2.530	144.8
		H27···O10	2.049	2.843	140.5
	DFT	H15···O14	1.560	2.483	150.3
		H27···O10	1.931	2.787	145.4
d-r-ξ	HF	H15···O14	1.676	2.524	145.5
		H16···O26	2.033	2.933	158.9
	DFT	H15···O14	1.547	2.477	151.1
		H16···O26	1.926	2.865	162.1

is also 0.152/HF and 0.134/DFT Å shorter in the s-w-η conformer than in the d-w-ξ conformer. The H16···O26 intermonomer IHB, present in *r* conformers, is the longest IHB, which provides an additional contribution to the better energy of the s-w-η conformer with respect to the s-r conformer.

Table 4 reports the distances of the H atom of the relevant OH from the sp^2 C atoms in the prenyl chain (C29 and C30), for the conformers in which the O–H···π interaction is present. Although this interaction cannot be specified by two atoms (as in the case of the other IHB considered here), the distance of the H atom from the two sp^2 C atoms is an indication of its strength. Comparison of the two calculation methods shows shorter values for DFT; it has however to be recalled that DFT tends to overestimate the strength of IHB and to give IHB length values that are usually shorter than the experimental ones.

Table 5 reports the C3-C9-C17 bond angle of the methylene bridge, which give an indication of the mutual orientation of the two rings. The value is practically constant for all the conformers and with both calculation methods.

Table 4. Distance of the H atom of the relevant OH from the two sp^2 carbon atoms of the prenyl chain, for the conformers in which the O–H···π interaction is present. In the indications of the method, HF stays for HF/6-31G(d,p) and DFT for DFT/B3LYP/6-31+G(d,p) results.

conformer	method	H···C distance considered	H···C (Å)
s-w-η	HF	H16···C29	2.253
		H16···C30	2.565
	DFT	H16···C29	2.071
		H16···C30	2.426
d-w-η	HF	H16···C29	2.354
		H16···C30	2.675
	DFT	H16···C29	2.122
		H16···C30	2.472
d-w-ξ	HF	H17···C29	2.356
		H17···C30	2.700
	DFT	H17···C29	2.142
		H17···C30	2.530
d-r-ξ	HF	H17···C29	2.291
		H17···C30	2.621
	DFT	H17···C29	2.111
		H17···C30	2.491

Table 5. C3-C9-C17 bond angle of the methylene bridge for the calculated conformers of the arzanol molecule. In the indications of the method, HF stays for HF/6-31G(d,p) and DFT for DFT/B3LYP/6-31+G(d,p) results.

conformer	C3-C9-C17 bond angle	
	HF	DFT
s-w-η	117.0	116.9
s-r	116.1	116.7
d-w-η	115.8	116.8
d-w-ξ	115.9	116.8
d-r-ξ	114.9	115.5

Table 6 reports the Mulliken charges on the O atoms and on the H atoms bonded to O atoms. These are the atoms that are responsible for intramolecular interactions like IHB and that are likely more responsible for interactions with the biological target. Only the HF/6-31G(d,p) and DFT/B3LYP/6-31+G(d,p) results are reported, because, since the MP2/6-31-G(d,p) calculations were performed as single points on the HF results, the MP2/6-31-G(d,p) values coincide with the HF values.

Table 7 reports the energy difference between the frontier orbitals (HOMO, highest occupied molecular orbital, and LUMO, lowest unoccupied molecular orbital). This difference enables prediction of molecular reactivity, as HOMO is related to the ionization energy and to the molecule's ability to act as nucleophile, while LUMO is related to the electron affinity and to the molecule's ability to act as electrophile. The HOMO-

Table 6. Mulliken charges on the O atoms and on the H atoms attached to O atoms, in the arzanol molecule. Results in vacuo.
In the indications of the method, HF stays for HF/6-31G(d,p) and DFT for DFT/B3LYP/6-31+G(d,p) results.

conformer	atom considered	Mulliken charge on the atom	
		HF	DFT
s-w-η	O8	-0.707365	-0.588744
	O10	-0.735396	-0.560747
	O12	-0.679136	-0.578976
	O14	-0.647666	-0.496619
	O19	-0.653887	-0.325948
	O23	-0.660911	-0.520814
	O26	-0.672030	-0.547368
	H15	0.427032	0.443110
	H16	0.373941	0.381995
	H17	0.419662	0.462219
	H27	0.415058	0.450784
s-r	O8	-0.712855	-0.573675
	O10	-0.682239	-0.531219
	O12	-0.679829	-0.572341
	O14	-0.648426	-0.499750
	O19	-0.652537	-0.322811
	O23	-0.635158	-0.512131
	O26	-0.674811	-0.550577
	H15	0.417009	0.431209
	H16	0.388551	0.413161
	H17	0.414772	0.453073
	H27	0.379286	0.388030
d-w-η	O8	-0.656723	-0.514779
	O10	-0.633424	-0.557046
	O12	-0.667445	-0.504259
	O14	-0.716717	-0.476604
	O19	-0.670141	-0.337483
	O23	-0.573884	-0.443220
	O26	-0.672945	-0.500494
	H15	0.417269	0.455753
	H16	0.368488	0.363322
	H17	0.361810	0.349656
	H27	0.394957	0.414006
d-w-ξ	O8	-0.658042	-0.509821
	O10	-0.700275	-0.567342
	O12	-0.680277	-0.507183
	O14	-0.633249	-0.480941
	O19	-0.670226	-0.337613
	O23	-0.573204	-0.440175
	O26	-0.671220	-0.489422
	H15	0.416691	0.455168
	H16	0.365550	0.358607
	H17	0.365474	0.365759
	H27	0.390888	0.398187
d-r-ξ	O8	-0.669515	-0.524904
	O10	-0.687022	-0.531314
	O12	-0.682596	-0.509573
	O14	-0.644771	-0.492396
	O19	-0.668583	-0.329844
	O23	-0.551014	-0.416150
	O26	-0.681918	-0.547997
	H15	0.417112	0.458194
	H16	0.393879	0.423300
	H17	0.366741	0.368328
	H27	0.374025	0.384688

Table 7. HOMO-LUMO energy difference for the calculated conformers of arzanol in vacuo.
In the indications of the method, HF stays for HF/6-31G(d,p) and DFT for DFT/B3LYP/6-31+G(d,p) results. The values from MP2/6-31-G(d,p) calculations coincide with the HF/6-31G(d,p) values because MP2/6-31-G(d,p) calculations were performed as single point on the optimized HF geometries.

conformer	HOMO-LUMO energy difference (kcal/mol)	
	HF	DFT
s-w-η	251.524	98.055
s-r	232.749	78.533
d-w-η	253.714	98.023
d-w-ξ	253.639	98.732
d-r-ξ	248.500	95.149

LUMO difference is particularly important for the study of biologically active molecules because it is one of the QSAR (Quantitative Structure Activity Relationships) descriptors. This difference is one of the features for which the results of DFT and other methods may differ dramatically; however, it is also known that the DFT results for this difference need to be taken with considerable caution, as they are often non-realistic [15].

Fig. 5 shows the shapes of the HOMO and LUMO molecular orbitals of the calculated conformers, comparing them in the HF/6-31G(d,p) and DFT/B3LYP/6-31+G(d,p) results. The shapes of each of these molecular orbital appear to be similar with the two methods, despite the high discrepancy in their energy difference due to the known tendency of DFT to give smaller values.

Fig. 6 shows the shapes of the four highest occupied molecular orbitals, usually considered as interesting for a better understanding of a molecule's behavior: the HOMO, the orbital with energy immediately lower than HOMO (HOMO–1), the one with energy immediately lower than HOMO–1 (HOMO–2) and the one with energy immediately lower than HOMO–2 (HOMO–3). It is interesting to note some similarities in the region of the molecule in which a certain MO is more present, depending on the geometry characteristics of the conformers. For instance, when the conformer involves an O–H···π interaction between the double bond of the prenyl chain and either H16 (η conformers) or H17 (ξ conformers), HOMO–3 is mostly distributed in the region of the prenyl chain.

Table 8 reports the energy difference of HOMO–1, HOMO–2 HOMO–3 with respect to HOMO.

Table 9 reports the dipole moment of the conformers of arzanol from HF/6-31G(d,p) and DFT/B3LYP/6-31+G(d,p) results (the MP2/6-31-G(d,p) values coincide with the HF/6-31G(d,p) because the MP2/6-31-G(d,p) calculations were performed as single point calculations on the HF optimized geometries). The dipole moment may be relevant for a compound's biological activity (e.g., anthracyclines show

anticancer activity only if their dipole moment is comparatively low, and the activity decreases as the dipole moment increases [21]). It may also be one of the QSAR descriptors, when the activity depends on the molecule's polarity.

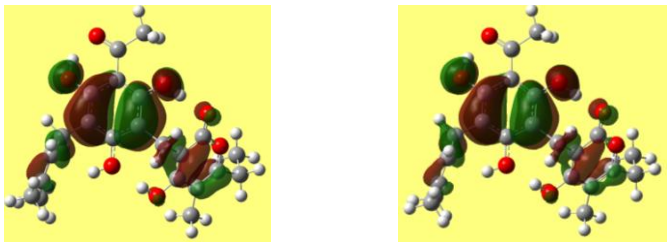

HF HOMO s-w-η DFT

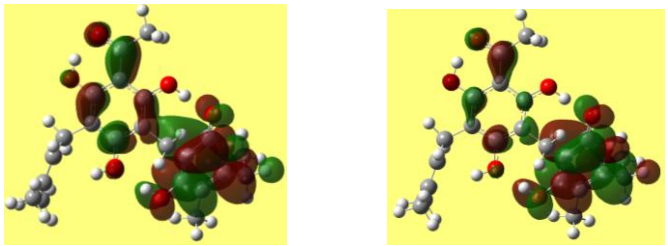

HF LUMO s-w-η DFT

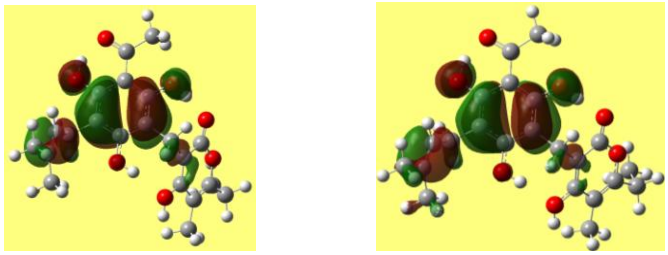

HF HOMO s-r DFT

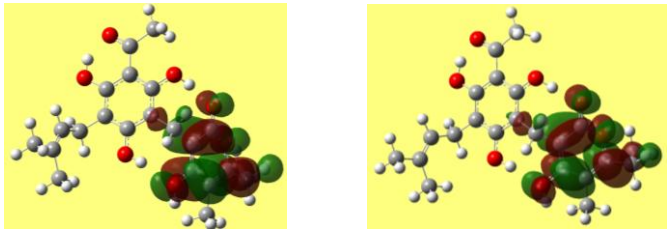

HF LUMO s-r DFT

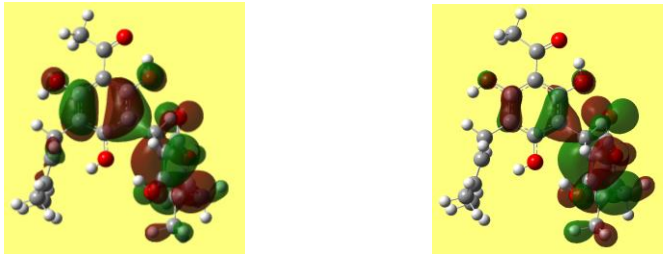

HF HOMO d-w-η DFT

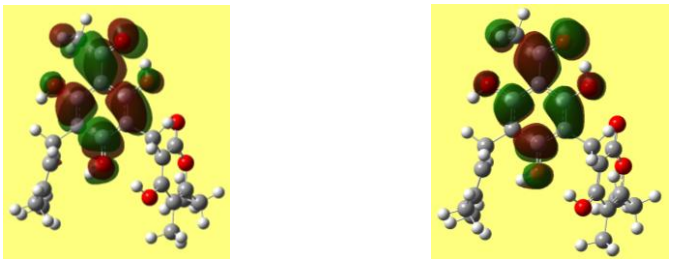

HF LUMO d-w-η DFT

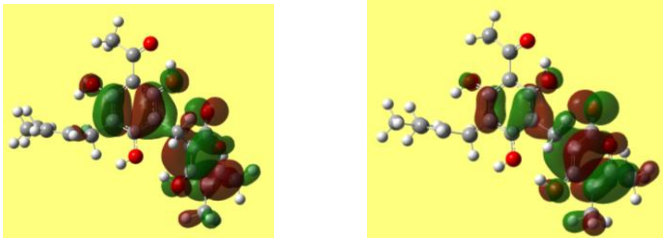

HF HOMO d-w-ξ DFT

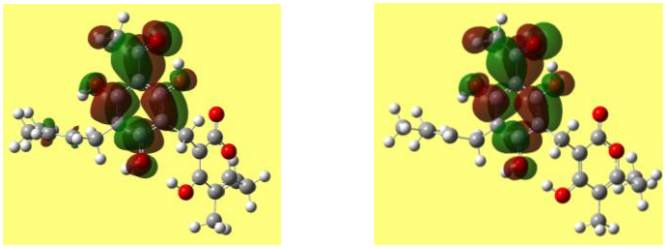

HF LUMO d-w-ξ DFT

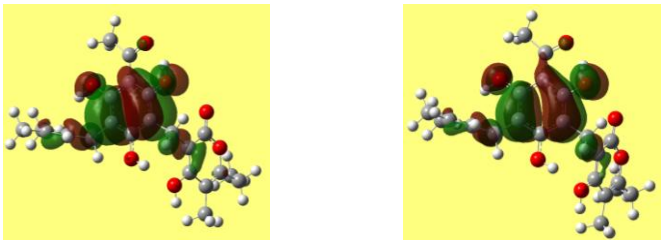

HF HOMO d-r-ξ DFT

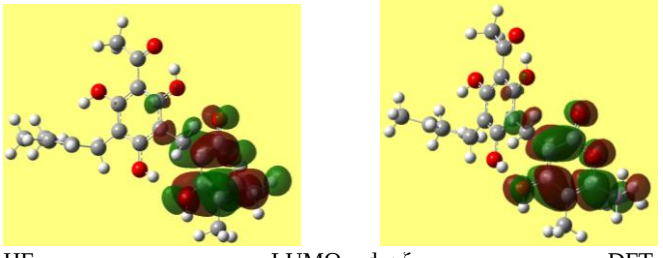

HF LUMO d-r-ξ DFT

Fig. 5. Shapes of the frontier molecular orbitals (HOMO and LUMO) of the calculated conformers of arzanol, in vacuo. For each of these orbitals, the HF/6-31G(d,p) and DFT/B3LYP/6-31-G+(d,p) results (respectively denoted as HF and DFT under the corresponding images) are compared.

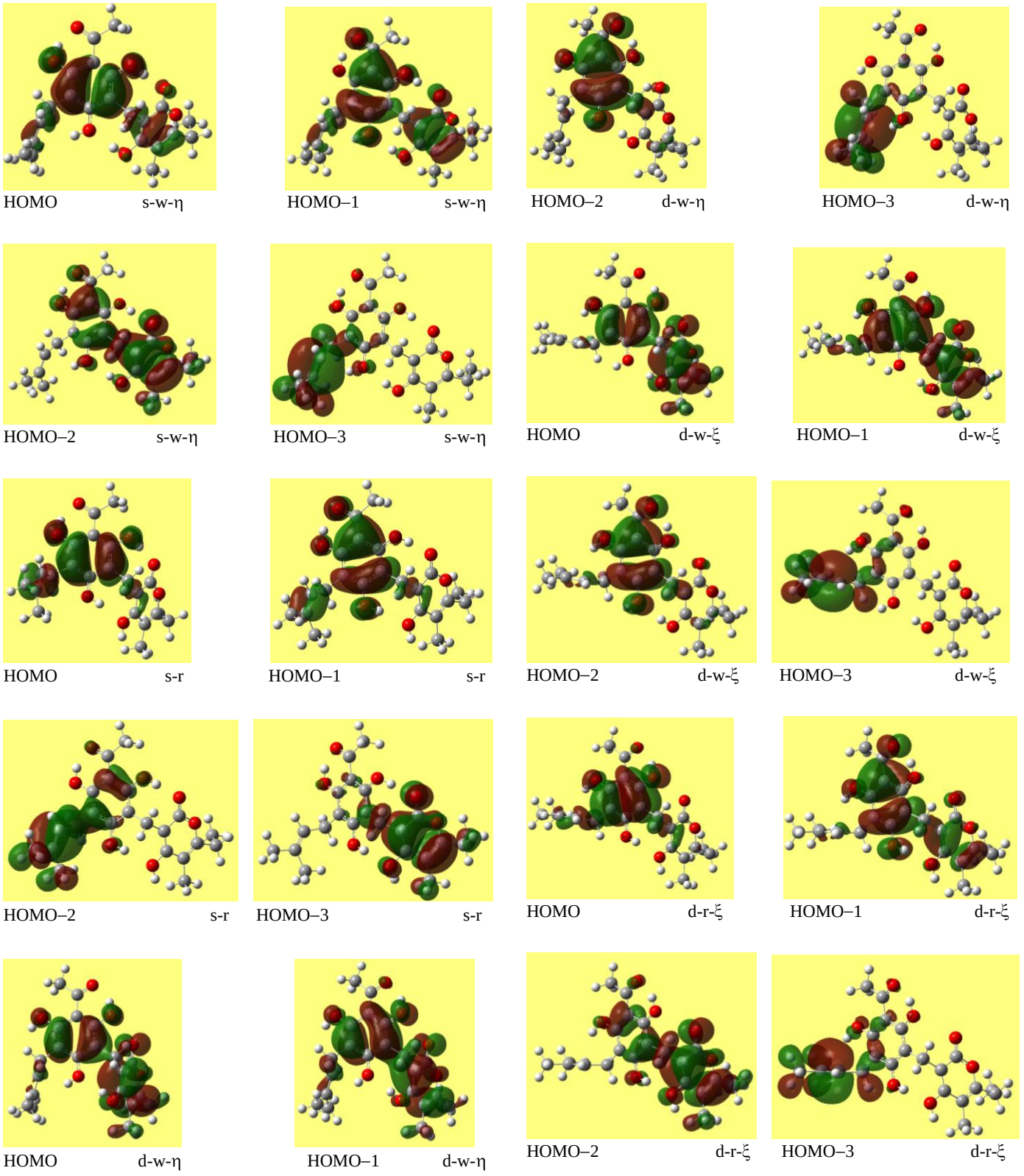

Fig. 6. Shapes of the four highest occupied molecular orbitals (HOMO, HOMO–1, HOMO–2 and HOMO–3) for the calculated conformers of arzanol. HF/6-31G(d,p) results in vacuo.

Table 8. Energy difference between HOMO and the higher energy occupied molecular orbitals immediately preceding it (HOMO–1, HOMO–2 and HOMO–3), for the calculated conformers of arzanol in vacuo. HF/6-31-G(d,p) and DFT/B3LYP/6-31-G+(d,p) results (respectively denoted as HF and DFT in the column headings).

conformer	MO considered	energy difference with HOMO (kcal/mol)	
		HF	DFT
s-w-η	HOMO–1	-14.3511	-13.4412
	HOMO–2	-18.0534	-15.6312
	HOMO–3	-35.8182	-26.8072
s-r	HOMO–1	-10.4794	-9.7013
	HOMO–2	-18.6684	-12.0670
	HOMO–3	-34.1490	-28.3885
d-w-η	HOMO–1	-5.5158	-5.7856
	HOMO–2	-17.8087	-18.2103
	HOMO–3	-45.0740	-28.9784
d-w-ξ	HOMO–1	-5.3150	-5.0201
	HOMO–2	-17.7020	-17.4510
	HOMO–3	-45.4819	-28.9344
d-r-ξ	HOMO–1	-10.8747	-10.5924
	HOMO–2	-18.1852	-15.4744
	HOMO–3	-36.6967	-27.2841

Table 9. Dipole moment of the calculated conformers of arzanol in vacuo, from HF/6-31-G(d,p) and DFT/B3LYP/6-31-G+(d,p) results (respectively denoted as HF and DFT in the column headings).

conformer	dipole moment (debye)	
	HF	DFT
s-w-η	7.2738	7.8278
s-r	12.8051	13.2462
d-w-η	9.8671	10.7005
d-w-ξ	9.9443	10.5139
d-r-ξ	9.8493	10.3311

B. Results in Solution

Fig. 7 shows the solvent accessible surface for the calculated conformers of arzanol, considering a solvent with a small radius (which better mimics the accessibility by water molecules).

Only the lowest energy conformer and the second lowest energy conformer were calculated in solution, because the relative energy of the others is too high for them to be interesting as potential contributors to the molecule's biological activity. Actually, also the s-r conformer does not appear to be interesting for the biological activity, because its relative energy in vacuo is much higher than the reference that is commonly taken to consider that a conformer may have some role in the biological activity (relative energy ≤ 3.5 kcal/mol); however, it was added to check for possible trends, such as a possible narrowing of the energy gap between the two conformers (a frequent phenomenon as the solvent polarity increases).

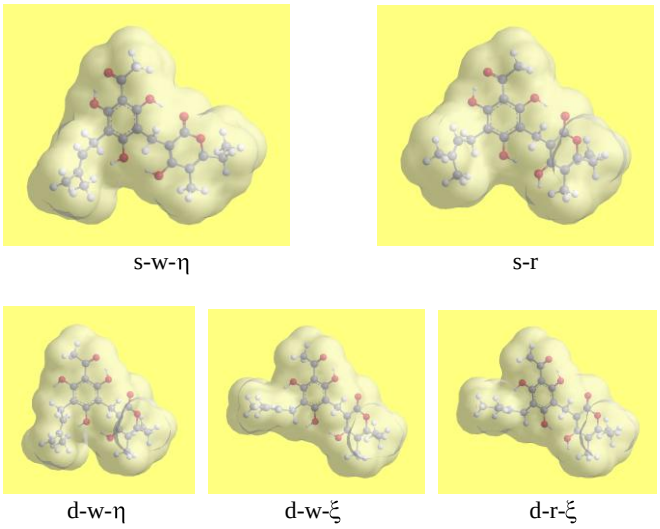

Fig. 7. Solvent accessible surface of the calculated conformers of the arzanol molecule, considering a solvent with small radius (1.4 Å).

The solvents selected cover the polarity range that is interesting for the media within a living organism, from non-polar (chloroform) to intermediate polarity (acetonitrile) and to high polarity (water). Furthermore, these solvents have different H-bonding abilities: chloroform cannot form H-bonds, acetonitrile can only be H-bond acceptor, while water can be both H-bond donor and H-bond acceptor. Considering solvents with different H-bonding abilities is important for molecules, like those of ACPL, that have sites that can be H-bond donors or acceptors. In the case or arzanol, all the O atoms can be H-bond acceptors and all the OH groups can be H-bond donors.

On reporting values, the media are indicated with the following acronyms: vac for *in vacuo*, chlrf for "in chloroform", actn for "in acetonitrile" and aq for "in water".

Table 10 compares the relative energies of the two conformers in different media. Similarly to what observed with ACPL in general, the energy gap between conformers decreases as the solvent polarity increases. The values for water solution show that also the s-r conformer may have some relevance for the biological activity, if one considers the cautious threshold of $\Delta E \leq 3.5$ kcal/mol for conformers to have a possibility of being involved in biological activities. However, arzanol will preferably be present in non-polar media within a living organism, as its octanol/water partition coefficient is 4.47673. Therefore, it can be expected that the role of the s-r conformer for biological activity would in any case be limited.

Table 11 compares the parameters of all the IHB of s-w-η and s-r in all the media considered (*in vacuo* and in the three solvents). The results for ACPL ([11], [22]) suggest that the

first IHB is maintained in solution, including water solution; however, the study of adducts with explicit water molecules – although computationally costly for a molecule like arzanol, with many centers to which water molecules can bind – could be relevant to verify whether this is the case even in the presence of the pyrone ring.

The fate of the IHB between the two rings may require additional investigations for inferences to be conclusive; however, their parameters in solution suggest that they are likely to be maintained in all the solvents, including water. The comparatively less accessibility to solvent molecules of the atoms forming these IHB, at least in some of the conformers, may also contribute to favor their permanence.

Table 10. Comparison of the relative energies of the s-w-η and s-r conformers of arzanol in different media. Full optimization HF/6-31G(d,p) results (PCM reoptimization for the results in solution).

conformer	relative energy (kcal/mol)			
	vac	chlrf	actn	aq
s-w-η	0.0000	0.0000	0.0000	0.0000
s-r	9.2452	5.9962	4.7379	2.2428

Table 11. Characteristics of the intramolecular hydrogen bonds of the s-w-η and s-r conformers in different media. HF/6-31G(d,p) results *in vacuo*, PCM HF/6-31G(d,p) results in solution.

conf-ormer	IHB	med-ium	O···H (Å)	O···O (Å)	OĤO
s-w-η	H17···O14	vac	1.658	2.612	150.0
		chlrf	1.657	2.512	146.4
		actn	1.656	2.513	146.6
		aq	1.662	2.517	146.2
	H15···O23	vac	1.795	2.744	170.9
		chlrf	1.787	2.737	171.0
		actn	1.784	2.734	170.9
		aq	1.786	2.733	169.5
	H27···O10	vac	1.897	2.826	164.8
		chlrf	1.906	2.831	163.6
		actn	1.912	2.835	162.7
		aq	1.939	2.841	157.2
s-r	H17···O14	vac	1.676	2.525	145.5
		chlrf	1.671	2.524	146.1
		actn	1.669	2.523	146.3
		aq	1.675	2.527	145.9
	H15···O23	vac	1.833	2.773	168.0
		chlrf	1.798	2.744	169.7
		actn	1.790	2.737	169.8
		aq	1.786	2.732	169.1
	H16···O26	vac	2.040	2.955	162.9
		chlrf	2.008	2.934	166.3
		actn	1.994	2.923	167.0
		aq	1.978	2.903	165.1

Table 12. Mulliken charges on the O atoms and on the H atoms attached to O atoms, in the arzanol molecule. HF/6-31G(d,p) results in vacuo (vac), chloroform (chlrf), acetonitrile (actn) and water (aq).. In the indications of the method, HF stays for and DFT for DFT/B3LYP/6-31+G(d,p) results.

conformer	atom considered	medium	Mulliken charge on the atom
s-w-η	O8	vac	-0.707365
		chlrf	-0.711259
		actn	-0.712899
		aq	-0.716311
	O10	vac	-0.735396
		chlrf	-0.730796
		actn	-0.728006
		aq	-0.722645
	O12	vac	-0.679136
		chlrf	-0.683955
		actn	-0.685721
		aq	-0.691952
	O14	vac	-0.647666
		chlrf	-0.663577
		actn	-0.669195
		aq	-0.683551
	O19	vac	-0.653887
		chlrf	-0.655077
		actn	-0.656447
		aq	-0.661150
	O23	vac	-0.660911
		chlrf	-0.683442
		actn	-0.692584
		aq	-0.711356
	O26	vac	-0.672030
		chlrf	-0.669188
		actn	-0.667737
		aq	-0.670907
	H15	vac	0.427032
		chlrf	0.426424
		actn	0.426075
		aq	0.425410
	H16	vac	0.373941
		chlrf	0.377129
		actn	0.378649
		aq	0.382847
	H17	vac	0.419662
		chlrf	0.416689
		actn	0.415670
		aq	0.417338
	H27	vac	0.415058
		chlrf	0.416133
		actn	0.416826
		aq	0.419572
s-r	O8	vac	-0.712855
		chlrf	-0.715426
		actn	-0.716372
		aq	-0.718377
	O10	vac	-0.682239
		chlrf	-0.682783
		actn	-0.682332
		aq	-0.687531
	O12	vac	-0.679829

		chlrf	-0.687798
		actn	-0.690591
		aq	-0.696968
	O14	vac	-0.648426
		chlrf	-0.666830
		actn	-0.672956
		aq	-0.686616
	O19	vac	-0.652537
		chlrf	-0.652100
		actn	-0.653348
		aq	-0.657748
	O23	vac	-0.635158
		chlrf	-0.666587
		actn	-0.678904
		aq	-0.703570
	O26	vac	-0.674811
		chlrf	-0.680097
		actn	-0.681727
		aq	-0.691537
	H15	vac	0.417009
		chlrf	0.422093
		actn	0.423181
		aq	0.424043
	H16	vac	0.388551
		chlrf	0.397234
		actn	0.400761
		aq	0.406823
	H17	vac	0.414772
		chlrf	0.412071
		actn	0.411263
		aq	0.413637
	H27	vac	0.379286
		chlrf	0.394971
		actn	0.401700
		aq	0.422750

Table 13. Comparison of the HOMO-LUMO energy difference of the s-w-η and s-r conformers of arzanol in different media. Full optimization HF/6-31G(d,p) results (PCM reoptimization for the results in solution).

conformer	HOMO-LUMO energy difference (kcal/mol)			
	vac	chlrf	actn	aq
s-w-η	251.524	252.459	252.265	252.164
s-r	232.749	242.677	246.159	250.056

Table 12 compares the Mulliken charges on the O atoms and on the H atoms bonded to O atoms for the s-w-η and s-r conformers in different media. The charges on the O atoms appear to become more negative as the solvent polarity increases, with the exception of O10 and O26 in the s-w-η conformer, likely because of their comparatively poorer accessibility by water molecules due to the steric effects of R′ and R″.

Table 13 compares the HOMO-LUMO energy difference of s-w-η and s-r in different media, and fig. 8 compares the shapes of the HOMO and LUMO orbitals of the two conformers in different media. The energy difference remains very similar across media. The shape of the HOMO orbital remains very similar across media, whereas there are noticeable differences in the shapes of the LUMO.

Table 14 compares the energy difference of the highest occupied molecular orbitals (HOMO−1, HOMO−2, HOMO−3,) with respect to HOMO, in different media.

Table 15 compares the dipole moment of the s-w-η and s-r conformers in different media. In both cases, the dipole moment increases as the solvent polarity increase.

Table 16 reports the thermodynamic quantities of the solution process: the solvent effect (free energy of solvation, ΔG_{solv}) and its electrostatic component (G_{el}). In the PCM method, ΔG_{solv} is the sum of an electrostatic component and a non-electrostatic component ($G_{non\text{-}el}$). ($G_{non\text{-}el}$) is not reported because it can be easily obtained as a difference ($G_{non\text{-}el} = \Delta G_{solv} - G_{el}$). The contributions to $G_{non\text{-}el}$ are reported in table 17 (the cavitation energy being the energy needed for the solute molecule to form a cavity in the continuum solvent, into which it gets embedded).

Table 14. Energy difference between HOMO and the higher energy occupied molecular orbitals immediately preceding it (HOMO−1, HOMO−2 and HOMO−3), for the s-w-η and s-r conformers of arzanol in different media. Full-optimization HF/6-31G(d,p) results with full PCM reoptimization for the calculations in solution.

conf	medium	orbital	energy difference with HOMO (kcal/mol)
s-w-η	vac	HOMO-1	-14.3511
		HOMO-2	-18.0534
		HOMO-3	-35.8182
	chlrf	HOMO-1	-13.3032
		HOMO-2	-16.7357
		HOMO-3	-31.2750
	actn	HOMO-1	-12.7259
		HOMO-2	-16.4972
		HOMO-3	-29.6875
	aq	HOMO-1	-11.8850
		HOMO-2	-15.9638
		HOMO-3	-26.8699
s-r	vac	HOMO-1	-10.4794
		HOMO-2	-18.6684
		HOMO-3	-34.1490
	chlrf	HOMO-1	-10.3790
		HOMO-2	-19.1955
		HOMO-3	-24.7301
	actn	HOMO-1	-10.1656
		HOMO-2	-18.9759
		HOMO-3	-21.7369
	aq	HOMO-1	-9.8268
		HOMO-2	-17.2377
		HOMO-3	-20.0113

Table 15. Comparison of the dipole moments of the s-w-η and s-r conformers of arzanol in different media. Full optimization HF/6-31G(d,p) results (PCM reoptimization for the results in solution).

conformer	dipole moment (debye)			
	vac	chlrf	actn	aq
s-w-η	7.2738	8.7754	9.3866	10.2257
s-r	12.8051	15.0891	15.9190	16.8250

Table 16. Thermodynamic quantities of the solution process of the s-w-η and s-r conformers of arzanol in different solvents. Full optimization HF/6-31G(d,p) results (PCM reoptimization for the results in solution).

conformer	quantity	quantity value (kcal/mol)		
		chlrf	actn	aq
s-w-η	ΔG_{sol}	1.46	7.73	-3.81
	G_{el}	-4.08	-5.73	-12.87
s-r	ΔG_{sol}	-1.76	3.19	-11.12
	G_{el}	-7.49	-10.52	-20.43

Table 17. Contributions to the non-electrostatic component of ΔG_{sol}. Full optimization HF/6-31G(d,p) results (PCM reoptimization for the results in solution).

conformer	energy contribution	value (kcal/mol)		
		chlrf	actn	aq
s-w-η	cavitation	35.89	42.68	49.71
	dispersion	-34.82	-34.53	-49.22
	repulsion	4.48	5.31	8.58
s-r	cavitation	36.18	43.01	50.05
	dispersion	-34.98	-34.68	-49.44
	repulsion	4.52	5.37	8.70

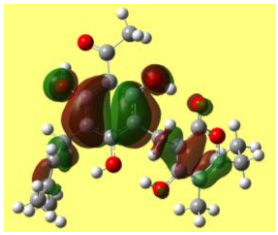
HOMO s-w-η vac

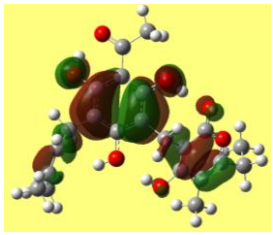
HOMO s-w-η chlrf

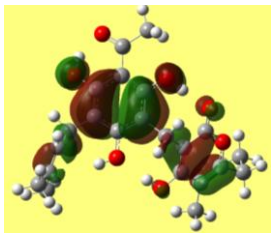
HOMO s-w-η actn

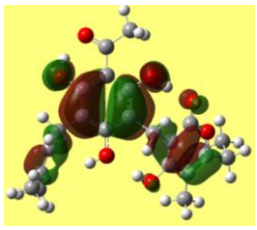
HOMO s-w-η aq

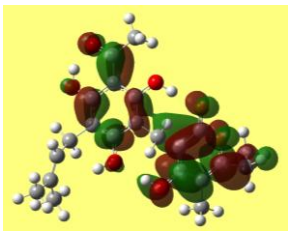
LUMO s-w-η vac

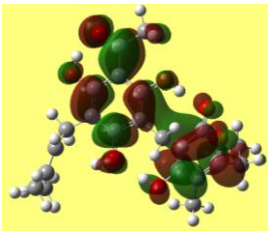
LUMO s-w-η chlrf

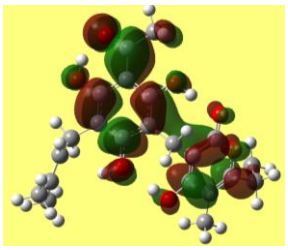
LUMO s-w-η actn

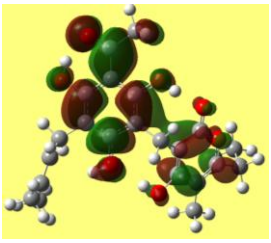
LUMO s-w-η aq

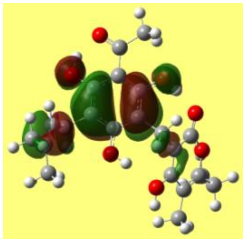
HOMO s- r vac

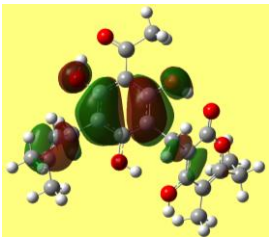
HOMO s- r chlrf

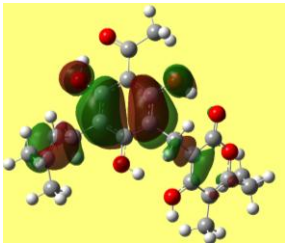
HOMO s- r actn

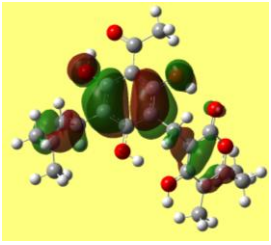
HOMO s- r aq

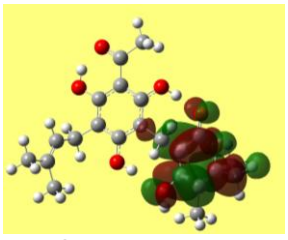
LUMO s-r vac

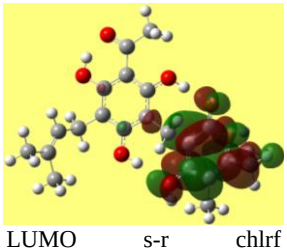
LUMO s-r chlrf

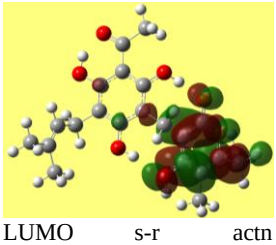
LUMO s-r actn

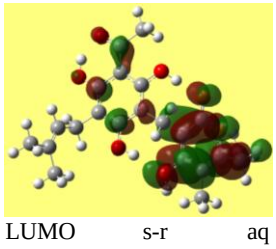
LUMO s-r aq

Fig. 8. Comparison of the shape of the HOMO and LUMO orbitals of the s-w-η and s-r conformers of arzanol in different media.
Full optimization HF/6-31G(d,p) results (PCM reoptimization for the results in solution).

IV. Conclusions

The computational study of the arzanol molecule falls in line with other case studies performed on selected ACPL molecules which appeared particularly interesting or representative of specific aspects, like caespitate ([23], [24]) and nodifloridin B ([25]–[27].

The results of the computational study of the arzanol molecule reported here highlight fair consistency with the general trends identified for ACPL [8–11]. In particular, they confirm:

- the importance of the stabilizing effect of the first IHB and the expectation that it remains in solution;
- the importance of the stabilizing effect of the IHB between the two rings;
- the similarity of the parameters of the three IHB in different media;
- the stabilizing effect of the O–H···π interaction;
- the narrowing of the energy gap between conformers as the medium polarity increases.

The fact that only one conformer is populated is also consistent with identified ACPL trends, as, for arzanol, s-w-η is the only possible conformer comprising all the stabilizing effects: presence of the first IHB; presence of two IHB between the two rings; presence of the O–H···π interaction; uniform orientation of the three phenol OH of the phloroglucinol moiety (which contributes ≈ 1 kcal/mol, [11]); and a number of C–H···O weaker H-bonds.

References

[1] G. Appendino, M. Ottino, N. Marquez, F. Bianchi, A. Giana, M. Ballero, O. Sterner, B. L. Fiebich and E. Munoz, "Arzanol, an Anti-inflammatory and Anti-HIV-1 Phloroglucinol r-Pyrone from *Helichrysum italicum* ssp. *microphyllum*", *Journal of Natural Products*, vol. 70, pp. 608-612. 2007.

[2] J. Bauer, A. Koeberle, F. Dehm, F. Pollastro, G. Appendino, H. Northoff, A. Rossi, L. Sautebin and O. Werz, "Arzanol; a prenylated heterodimeric phloroglucinyl pyrone; inhibits eicosanoid biosynthesis and exhibits anti-inflammatory efficacy *in vivo*", *Biochemical Pharmacology*, vol. 81, pp. 259–268, 2011.

[3] A. Rosa, F. Pollastro, A. Atzeri, G. Appendino, M. P. Melis, M. Deiana, A Incani, D. Loru and M. A. Dessì, "Protective role of arzanol against lipid peroxidation in biological systems", *Chemistry and Physics of Lipids*, vol. 164, pp. 24–32, 2011.

[4] C. Cappelli, B. Mennucci and S. Monti, "Environmental effects on the spectroscopic properties of gallic acid", *The Journal of Physical Chemistry A*, vol. 109, pp. 1933–1943, 2005.

[5] C. A. Gomes, T. Girão da Cruz, J. L. Andrade, N. Milhazes, F. Borges, and M. P. M. Marques, "Anticancer activity of phenolic acids of natural or synthetic origin: a structure-activity study", *Journal of Medicinal Chemistry*, vol. 46, pp. 5395–54012003.

[6] E. Sergediene, K. Jonsson, H. Szymusiak, B. Tyrakowska, I. C. M. Rietjens and N. Cenas, "Prooxidant toxicity of polyphenolic antioxidants to HL-60 cells: description of quantitative structure-activity relationships", *FEBS Letters*, vol. 462, pp. 392–396, 1999.

[7] G. Alagona and C. Ghio, "Plicatin B conformational landscape and affinity to copper (I and II) metal cations. A DFT study", *Phys Chem Chem Phys*, vol. 11, pp. 776–790, 2009.

[8] S. Peuchen, J. P. Bolanos, S. J. R. Heales, A. Almeida, M. R. Duchen, J. B. Clark, "Interrelationships between astrocyte function, oxidatice stress and antioxidant status within the central nervous system", *Progress Neurobiology*, vol. 52, pp. 261–281, 1997.

[9] F. Facchinetti, V. L. Dawson and T.M. Dawson, "Free radicals as mediators of neuronal injury", *Cell. Mol. Neurobioogyl*, vol. 18, pp. 667–677, 1998.

[10] L. Mammino and M. M. Kabanda, "A study of the intramolecular hydrogen bond in acylphloroglucinols", *Journal of Molecular Structure* (*Theochem)*, vol. 901, pp. 210–219, 2009.

[11] L. Mammino and M. M. Kabanda, "A computational study of the effects of different solvents on the characteristics of the intramolecular hydrogen bond in acylphloroglucinols", *The Journal of Physical Chemistry A*, vol. 113, no. 52, pp. 15064–15077, 2009.

[12] L. Mammino and M. M. Kabanda, "Computational study of the patterns of weaker intramolecular hydrogen bonds stabilizing acylphloroglucinols", *International Journal of Quantum Chemistry*, vol. 112, pp. 2650–2658, 2012.

[13] M. M. Kabanda and L. Mammino, "The conformational preferences of acylphloroglucinols – a promising class of biologically active compounds", *International Journal of Quantum Chemistry*, vol. 112, pp. 3691–3702, 2012.

[14] S. G. Chiodo, M. Leopoldini, N. Russo and M. Toscano, "The inactivation of lipid peroxide radical by quercetin: A theoretical insight", *Phys Chem Chem Phys*, vol. 12, pp. 7662–7670, 2010.

[15] V. Barone, M. Cossi and J. Tomasi, "Geometry Optimization of Molecular Structures in Solution by the Polarizable Continuum Model", *Journal of Computational Chemistry*, vol. 19, pp. 404–41, 1998.

[16] C. Amovilli, V. Barone, R. Cammi, E. Cancès, M. Cossi, B. Mennucci, C. S. Pomelli and J. Tomasi, "Recent Advances in the Description of Solvent Effects with the Polarisable Continuum Model", *Advances in Quantum Chemistry*, vol. 32, pp. 227–259, 1999.

[17] J. Tomasi, R. Cammi, B. Mennucci, C. Cappelli and S. Corni, "Molecular properties in solution described with a continuum solvation model", *Phys. Chem. Chem. Phys*., vol. 4, pp. 5697–5712, 2002.

[18] J. Tomasi, B. Mennucci and R. Cammi, "Quantum mechanical continuum solvation models", *Chemical Reviews*, vol. 105, pp. 2999–3093, 2005.

[19] M. J. Frisch, *et al*. GAUSSIAN 03, Revision D.01, Gaussian, Inc., Pittsburgh, PA, 2003.

[20] https://www.wiki.ed.ac.uk/display/EaStCHEMresearchwiki/How+to+analyse+the+orbitals+from+a+Gaussian+calculation

[21] S. N. Bushelyev and N. F. Stepanov, *Elektronnaya Struktura y Biologhicheskaya Aktivnost Molecul*. Khimiya, Snaye, Moscow, 1989.

[22] L. Mammino and M. M. Kabanda, "Adducts of acylphloroglucinols with explicit water molecules: Similarities and differences across a sufficiently representative number of structures", *International Journal of Quantum Chemistry*, vol. 110, no. 13, pp. 2378–2390, 2010.

[23] L. Mammino and M. M. Kabanda, "Model structures for the study of acylated phloroglucinols and computational study of the caespitate molecule", *Journal of Molecular Structure* (*Theochem)* vol. 805, pp. 39–52, 2007.

[24] L. Mammino and M. M. Kabanda, "The geometric isomers of caespitate: a computational study in vacuo and in solution". *International Journal of Biology and Biomedical Engineering*, vol. 1, no. 6, 114–133, 2012.

[25] L. Mammino, M.M. Kabanda, "Computational study of nodifloridin-A and nodifloridin-B, with highlight of the peculiarities of acylated phloroglucinol derivatives", in C. A. Bulucea, V. Mladenov, E. Pop, M. Leba and N. Mastorakis (Eds), *Recent Advances in Biology, Biophysics, Bioengineering and Computational Chemistry*. WSEAS Press, 2009, pp. 58–63.

[26] L. Mammino and M.M. Kabanda, "Computational study of nodifloridin A and nodifloridin B in vacuo and in water solution", *WSEAS Transactions on Biology and Biomedicine*, vol. 6, no. 4, pp. 79–88, 2009.

[27] L. Mammino, "Computational study of ring-shaped dimers of nodifloridin B", in S. Oprisan, A. Zaharim, S. Eslamian, M. S. Jian, C. A. F. Ajub and A. Azami, Eds., *Advances in Environment, Computational Chemistry and* Bioscience, WSEAS, 2012, pp. 43–48.